

## Modeling the vibration of UAV camera position with DC Servo Motor (DCSM) and PID Controller

G.N Jola<sup>1</sup>, B.E. Zakka<sup>2</sup>, Sarah N. Aarih<sup>3</sup>

*Electrical Electronics Engineering Department Federal Polytechnic Bauchi, Nigeria<sup>2</sup>*

*Computer Science Department Federal Polytechnic Bauchi, Nigeria<sup>1</sup>*

*National Mathematical Centre, Abuja, Nigeria<sup>3</sup>*

---

**Abstract:** UAV in flight make varieties of vibration frequencies, as a result the images/video received from UAV cameras jitters and are not appealing due to the unstable motion of the camera holder. To address these issues, the camera level on the UAV has to be stationary, thus in this work the vibration was modeled as external disturbance acting on the camera to make it deviate from the reference set point. Inertia Measurement Unit (IMU) attached to the camera detect these vibrations from the UAV with respect to its translational and rotational dynamics. In addition, random noise was added to the system as a result of air drag forces acting on the camera from random directions. The camera itself was mounted on the UAV via a servo motor which act as the actuator. The actuator made it possible to set the reference camera positions. To minimize the layer of deviation, a PID controller was designed to counter the disturbances and keep the camera in relatively stable position. Thus, the output of the system is the camera position while the disturbance in the system is the vibration from the UAV. The overall system was modeled and simulated in MATLAB/SIMULINK environment. The response of the system to various kinds of inputs (reference positions) in the faces of different kinds of vibrations (external disturbances), with and without the controller was analyzed.

**Key Words:** vibration frequencies, jitters, unstable motion, reference set point, actuator.

---

### 1.0 Introduction

Unmanned aerial vehicles, UAV is the name given to vehicles that fly with no human controller on board, (Eisenbeiss, 2004). Interest in the development of UAVs were strongly motivated by military applications in the 1970s when some nations began looking for cheap and effective means for surveillance, reconnaissance and penetration of hostile terrain without endangering a pilot's life or other expensive machines (Eisenbeiss, 2004). These flying missions would also benefit from a smaller, covert vehicle compared to a manned aircraft. Engineers in the United States started experimenting with smaller, slower, cheaper UAVs that mimicked large model airplanes. Progress in this field was achieved over the years as these vehicles became larger and more capable, leading to a successful, wide deployment in the mid-90s, and due to their reconnaissance and tactical capabilities, UAVs are now a major component of the global war on terrorism.

Although UAVs were initially deployed for military missions, due to their extreme flexible nature they are increasingly being adopted for civil applications including firefighting, pipeline surveillance, law enforcement, assessment of natural disasters and environmental monitoring. ([www.lumenera.com](http://www.lumenera.com)). It is usual for unmanned aerial vehicles to carry payloads that make them useful in any application area. The payload is the weight a drone or unmanned aerial vehicle (UAV) can carry. It is usually counted outside of the weight of the drone itself, and includes anything additional to the drone; such payloads include high and low resolution cameras for still image or video capture, day and night reconnaissance equipment, high power radar, gyro stabilized, electro optical signals, meteorological, relay communications, navigation signals), warfare machinery, Electronic Support Measure (ESM), Electronic Counter Measure (ECM), Electronic Counter-Countermeasure (ECCM), weapons cargo (leaflets, supplies), and generally any equipment required for the mission the UAV is designed. (Gupta et al., 2013).

Aerial vehicles usually carry cameras to capture outside scenes in real-time. However, due to its size and structure limitation captured images jitters as a result of the vibration and wind resistance which produces undesirable effects on images /videos obtained. The poor quality of these images may cause the video not to be useful and reliable to guarantee the success of the mission. Thus the necessity of capturing stable images from UAV camera is invaluable because of its wide application and usage in areas such as for surveillance, target tracking, navigation and localization tasks. Also human operators often track and observe environments via live video images from UAVs. Therefore recognizing targets or landmarks is likely to fail when vibrations cause defocusing and blurriness in images. Thus to obtain clean images the camera need be stabilized.

### 1.1 Problem Statement

UAVs are equipped with cameras for capturing images which are used for immediate observation, object detection and tracking. However, due to either mechanical vibrations caused by the engine, atmospheric turbulence or motion of the vehicle, such images received from mobile UAV cameras suffer shaky and blurry effect and hence not clear. This work proposes an image stabilization technique which stabilizes the camera position in a stationary mode so as to obtain a more stable and clearer image.

### 1.2 Aim

The aim of this research work is to design a controller whose responsibility is to control the camera mounted on a UAV device keeping its position stationary despite the jitters and disturbances resulting from vibrations and irregular motion of the vehicle.

## 2.0 Literature Review

In this chapter relevant literature works carried out by various researchers are presented.

Vazquez et al. (2009), presented a real-time smoothing methodology for the stabilization of videos captured from small robotic helicopter platforms. It uses Lucas–Kanade feature tracker to detect the regions and then estimate the transformation between two consecutive frames. Unintended motion compensation is accomplished by adjusting for extra rotation and displacements that generate vibrations.

In a similar work, Hu et al (2007) developed a method removing the shaky frames from video images, so that the reconstructed output is a stabilized video with better visual quality than the original. In the work a so called the scale invariant features (SIFT) to estimate the camera motion. Also, unwanted vibrations were separated from the intentional camera motion by a combination of the Gaussian kernel filtering and parabolic fitting.

Wang et al., (2011) also reported a work on real-time video stabilization for unmanned aerial vehicles. The stabilizations task was achieved in three steps: The key points are located based on FAST corner detection and preliminarily matched. Secondly, the matched key points are then involved for estimation of affine transform to reduce false matching key points and thirdly motion estimation was performed based on affine transform model while the compensation for vibration was conducted based on Spline smoothing

In a similar work by Windau and Itti (2011), a real-time video image stabilization system (VISS) was developed for aerial robots. Its architecture combines four independent stabilization layers. Layer 1 detects vibrations via an inertial measurement unit (IMU) and performs external counter movements with a motorized gimbal. Layer 2 damps vibrations by using mechanical devices. The internal optical image stabilization of the camera represents Layer 3, while Layer 4 filters the remaining vibrations using software.

Manohar and Ananda, presented a work titled the design, simulation and development of two axes gimbal for holding and controlling the position of camera in Micro Aerial vehicle. The gimbal mechanism was employed to keep the camera towards target position by compensating the disturbances and vibrations caused by MAV while tracking target. While MAV was navigating with a bank by any angle, the gimbal rotates with help of servo motors to keep the camera focused on the target. The camera position was adjusted along the three axes named as roll, pitch and yaw axes by using three servo motors. Positional encoders were used as the feedback element to measure and stabilize the orientation of gimbal.

The three types of approach to stabilize images from video are Optical Image Stabilization (OIS), Mechanical Image Stabilization (MIS) and Digital Image Stabilization (DIS)

## 3.0 Methodology

This chapter presents the structure of the control system to be implemented and how the different blocks of the system are modeled. See figure 1.

The mathematical model for the position control of the UAV camera will be developed using dc motor as the actuator. The total torque on the system will be a combination of rotor torque, viscous torque and the external torque. The vibration model from UAV quadcopter will be the extracted from quadcopter dynamics as functions of their respective accelerations in both the translational and rotational motions. Random noise will also be modeled and added to the system. Having obtained the combined system model, PID will be introduced of which the design for optimum parameters and tuning will be carried out using MATLAB/SIMULINK software. Different simulation scenarios were created to test different kinds of disturbances.

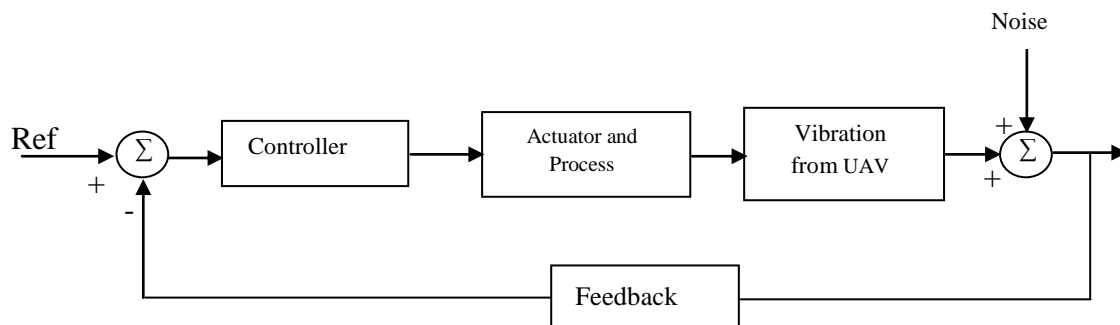


Figure 1: Structure of the control system

### 3.1 Actuator and Process Model

DC servo motor was used as the actuating device on which the UAV camera was mounted. Servo motors are known to have precise angular position and have a quick response when embedded into feedback control system. The differential equations and the Laplace domain transfer function model of the system dc motor with camera as load will be developed and PID controller will be designed to keep the camera position at the desired point irrespective of the disturbance torque (resulting from vibrations caused by the UAV motion) on the camera. The electric equivalent circuit of the armature and the free-body diagram of the rotor are shown in the following figure 2.

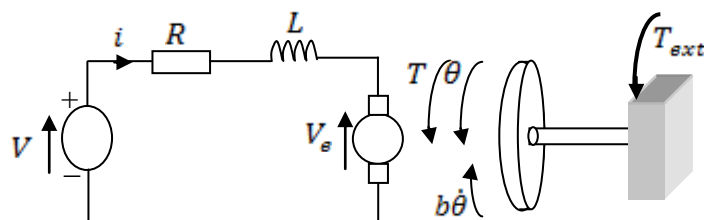


Figure 2. Motor equivalent circuit (Source: [1])

Where,  $R$  = Armature resistance,  $L$  = Inductance of the coil,  $V_g$  = Back emf  
 $i(t) = i$  = Armature current,  $K_g$  = Electromotive force constant,  $K_t$  = Motor constant  
 $\theta$  = Angular speed,  $\omega$  = Angular velocity,  $J$  = Moment of inertia of the motor  
 $b$  = Viscous force constant,  $T_{rotor}$  = Rotor torque,  $T_{ext}$  = External torque

### 3.2 Mathematical modeling of dc motor as actuator

The permanent magnets in the motor induce the following back emf  $V_g$  in the armature:

$$V_g = K_g \omega = K_g \dot{\theta} \quad (1)$$

The motor produces the following torque, which is proportional to the motor current  $i(t)$ :

$$T = K_t i(t) \quad (2)$$

Assuming there are no electromagnetic losses and no mechanical losses: mechanical power is equal to the electrical power

$$T \omega = V_g i(t) \quad (3)$$

Making substitution by equations (1) and (2)

$$K_t i(t) \omega = K_g \omega i(t), \text{ Hence, } K_t = K_g = K \quad (4)$$

From the Kirchhoff's law voltage, in the armature circuit:

$$V = Ri(t) + L \frac{di(t)}{dt} + V_g \quad (5)$$

From the Newton's Law, total torque  $T = T_{rotor} + T_{viscous} + T_{ext}$

$$T = J_m \ddot{\theta} + b \dot{\theta} + T_{ext} \quad (6)$$

**3.3 The Laplace domain transfer function model**

The main variables of the system are:

$V \rightarrow$  input of the system

$\theta \rightarrow$  output of the system

$T_{ext} \rightarrow$  disturbance of the system

From equation (5) and equation (1)

$$V = Ri(t) + L \frac{di(t)}{dt} + V_g = Ri(t) + L \frac{di(t)}{dt} + K\omega \tag{7}$$

Applying Laplace transform

$$V(s) = R.I(s) + Ls.I(s) + K.\Omega(s)$$

$$V(s) - K.\Omega(s) = (Ls + R).I(s)$$

$$I(s) = \frac{V(s) - K.\Omega(s)}{(Ls + R)} = [V(s) - K.\Omega(s)].\frac{1}{(Ls + R)} \tag{8}$$

$$\text{From equation (2), } T(s) = K.I(s) \tag{9}$$

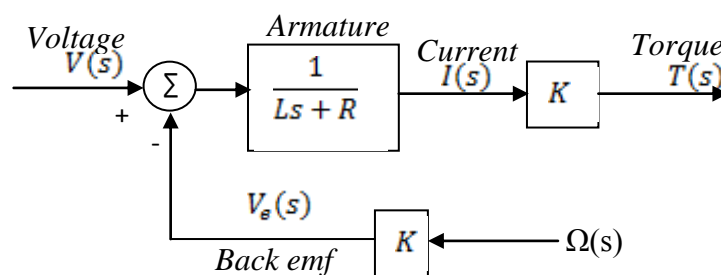


Figure 3: Open-loop transfer function block for motor torque

From equation (6),  $T = J\ddot{\theta} + b\dot{\theta} + T_{ext}$

Applying Laplace transform

$$T(s) = Js^2.\theta(s) + bs.\theta(s) + T_{ext}(s)$$

$$T(s) - T_{ext}(s) = s.(Js + b).\theta(s)$$

$$\theta(s) = [T(s) - T_{ext}(s)].\frac{1}{(Js + b)}.\frac{1}{s} \tag{10}$$

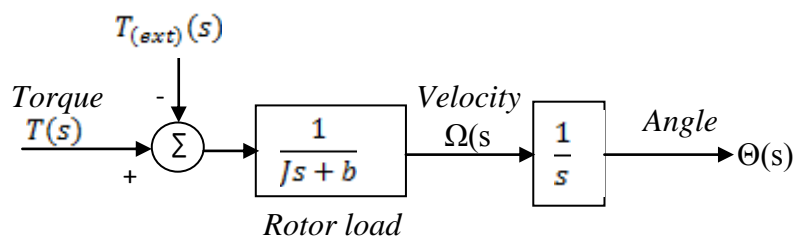


Figure 4: Open-loop transfer function block for camera position

Combining the two block diagrams, and assuming from equation (1)  $K.\omega = K\dot{\theta}$ , then from Laplace  $K.\Omega(s) = K.s.\theta(s)$ , we get the open-loop equivalent block diagram of the system in figure 5.

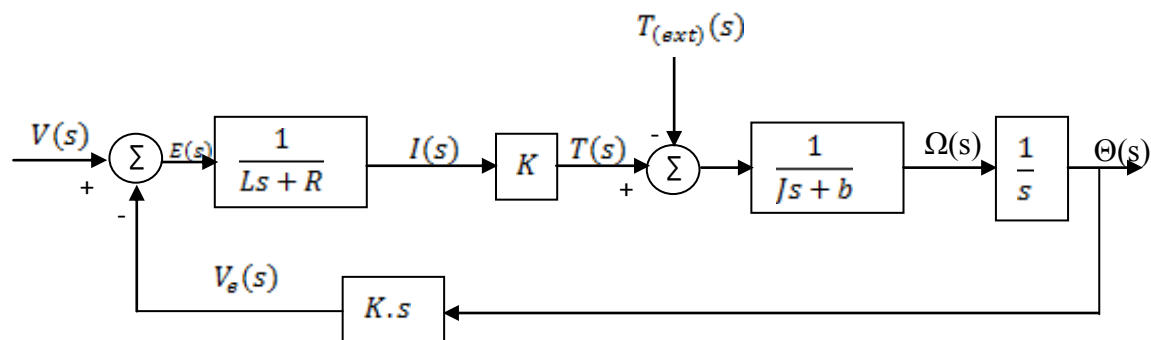


Figure 5: Close-loop transfer function block for the dc motor

$L/R$  is the electrical time constant, and  $J/b$  is the mechanical time constant. Usually  $L/R \ll J/b$ , so we can assume  $(Ls + R) \rightarrow R$ . With this consideration, we obtain the simplified block diagram of figure 6.

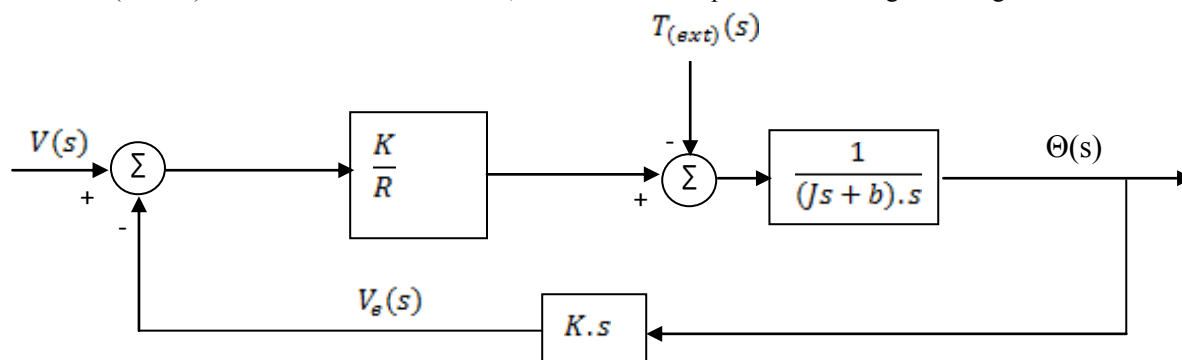


Figure 6: Simplify open-loop transfer function

### 3.4 UAV Vibration model

The dynamics of a UAV with respect to the earth inertial frame (E-frame) and the body-fixed frame of the vehicle (B-frame) as the two coordinate systems are to be considered and this is shown in figure 7. The two co-ordinates are related through three successive rotations such as the:

- Roll: Rotation of  $\phi$  about the x- body axis
- Pitch: Rotation of  $\theta$  around the y- body axis
- Yaw: Rotation of  $\psi$  around the z- body axis

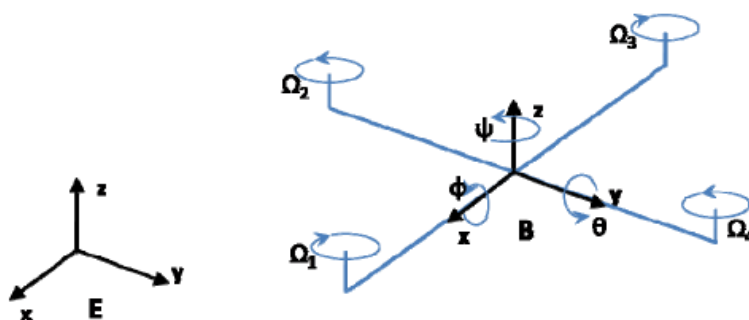


Figure 7: Quadcopter dynamic configuration

The quadrotor dynamic model presented in Pipatpaibul (2011) will be adopted. However, the vibrations from the UAV dynamics will be extracted using the quadrotor UAV motions defined by the equations of motion given in (11).

$$\begin{aligned}
 m\ddot{X} &= -\sin\theta \cos\phi \sum_{i=1}^4 [b\Omega_i^2] \\
 m\ddot{Y} &= \sin\phi \sum_{i=1}^4 [b\Omega_i^2] \\
 m\ddot{Z} &= -mg + \cos\theta \cos\phi \sum_{i=1}^4 [b\Omega_i^2] \\
 I_{xx}\ddot{\phi} &= \dot{\theta}\dot{\psi}(I_{yy} - I_{zz}) - \dot{\theta}\Omega_r J_r + lb(-\Omega_2^2 + \Omega_4^2) \\
 I_{yy}\ddot{\theta} &= \dot{\theta}\dot{\psi}(I_{zz} - I_{xx}) + \dot{\theta}\Omega_r J_r + lb(-\Omega_1^2 + \Omega_3^2) \\
 I_{zz}\ddot{\psi} &= \dot{\theta}\dot{\phi}(I_{xx} - I_{yy}) + \dot{\psi}\Omega_r J_r + \sum_{i=1}^4 [(-1)^i d\Omega_i^2]
 \end{aligned} \tag{11}$$

### 3.4.1 UAV motion with vibrations

The motion of the UAV is a combination of one of the translations or rotations in a chosen direction as presented below.

### 3.4.2. Z-direction Translation

To translate in the +Z direction, from hovering, rotor speed is increased equally to each rotor and vice versa in the -Z direction. Changes in rotor angular momentum in each pairs are equal and thus be canceled out. Figure 8 illustrates the concept of a vertical translation.

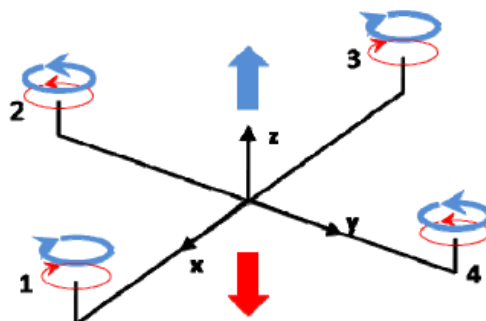


Figure 8. Z-direction translation

### 3.4.3 X-direction Translation and Pitching Motion

Since quadrotors are highly coupled, rotation in certain angles results in translation in a direction and that is fundamentally how a quadrotor UAV translates. This is also true to the pitching motion. Starting from hover, increasing rotor speed in rotor 3 and decreasing in rotor 1 while maintaining speeds in rotor 2 and 4 results in rotation in the  $+\theta$  direction and translation in the +X direction of Earth frame and vice versa. Note that at this point the quadrotor UAV tilts in a small angle and thrust are approximately equal to weight, thus no translation in the Z direction. This is illustrated in Figure 9.

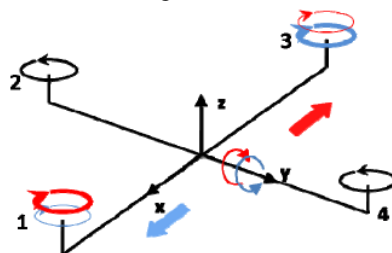


Figure 9. X-direction Translation and Pitching Motion

### 3.4.4 Y-direction Translation and Rolling Motion

Similar to pitching, rolling is coupled with the Y direction translation. In this case, starting from hover, increasing the rotor speed in rotor 4 and decreasing in rotor 2 while maintaining speeds in rotor 1 and 3 results

in rotation in  $+\theta$  direction and translation in  $-Y$  direction of the Earth frame and vice versa. This is also depicted in Figure 10.

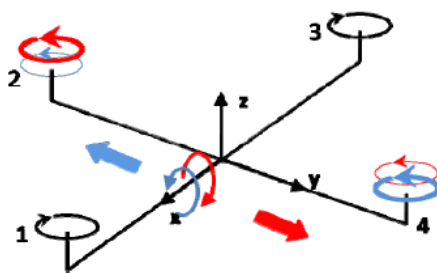


Figure 10. Y-direction Translation and Rolling Motion

### 3.4.5 Yaw Rotation

Yawing is similar to vertical translation in that the motion is not coupled. Instead of cancelling out rotor angular momentum, thrust is balanced to maintain altitude in this case. To perform a pure yaw motion, starting from hover, increasing the speed in rotor 2 and 4 while decreasing speeds in rotor 1 and 3 results in body rotation in  $+\varphi$  direction and vice versa. See Figure 11 for more details.

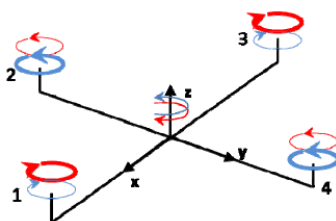


Figure 11. Yaw Rotation

### 3.5 Noise Model and Body Damping

A random noise model of the form given below will be used.

$$\text{Noise}(t) = 10 \times 10^{-9} \times 2 \times \text{noise\_level} \times (\text{random\_number} - 0.9) \tag{12}$$

Let  $D(t)$  be the vibration function from the UAV and  $d_0$  be the camera body damping coefficient.

Then,

$$\text{camera\_position\_noise} = d_0 \frac{d(\text{Noise})}{dt} \tag{13}$$

$$\text{camera\_position\_vibration} = d_0 \frac{d(D(t))}{dt} \tag{14}$$

The open loop transfer function of the system is now as shown in figure 12.

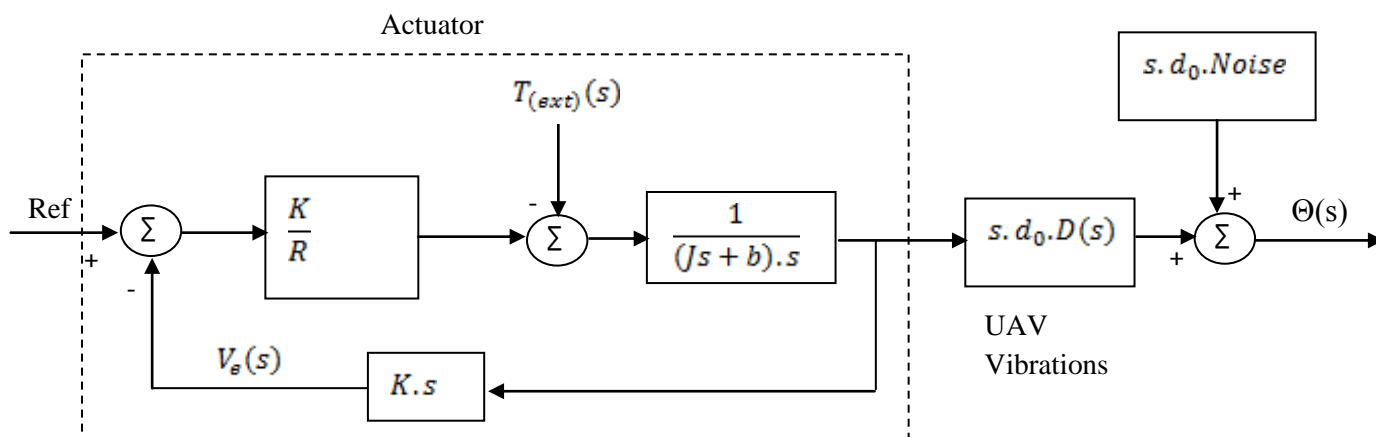


Figure 12: open-loop transfer function of the system

### 3.6 Close loop Model with Feedback and PID Controller blocks

To control the position of the motor, the system must be closed with a feedback, and a controller C(s) has to be added as shown in figure 13

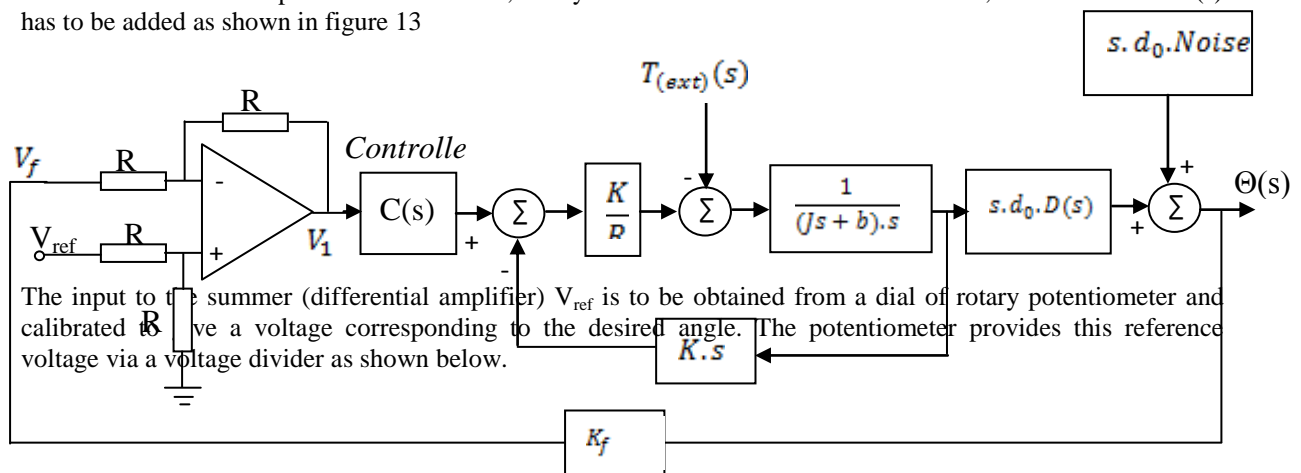


Figure 13: Close-loop transfer function of the system with controller

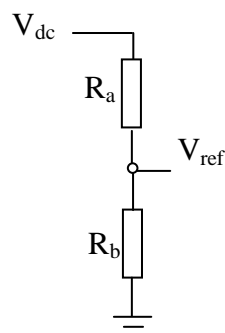


Figure 14: Potentiometer circuit

Where

$$V_{ref} = \frac{R_b}{R_a + R_b} \cdot V_{dc} \tag{15}$$

Similarly, the feedback sensor is attached to another rotary potentiometer whose gain is  $K_f$

From figure 13, the differential amplifier provides the error voltage  $V_1 = e$ , while  $V_{ref} = \theta_d(s)$ .

$$V_1 = \frac{1+R_2/R_1}{1+R_3/R_4} \cdot V_{ref} - \frac{R_2}{R_1} \cdot V_f \tag{16}$$

But  $V_f = K_f \cdot V_{ref}$

Hence,

$$V_1 = \frac{1+R_2/R_1}{1+R_3/R_4} \cdot V_{ref} - \frac{R_2}{R_1} \cdot K_f \cdot V_{ref} \tag{17}$$

In a balance state,  $V_1 = 0$ ;

Therefore,  $\frac{1+R_2/R_1}{1+R_3/R_4} = \frac{R_2}{R_1} \cdot K_f$

$$K_f = \frac{1+R_1/R_2}{1+R_3/R_4} \tag{18}$$

$R_1, R_2, R_3$  and  $R_4$  will be selected so that when  $\theta_d = 0, V_{ref} = 0$  and when  $\theta_d = 360^\circ, V_{ref} = V_{dc}$ .

Assuming a unity feedback system, figure 13 can be redrawn as shown in figure 15.



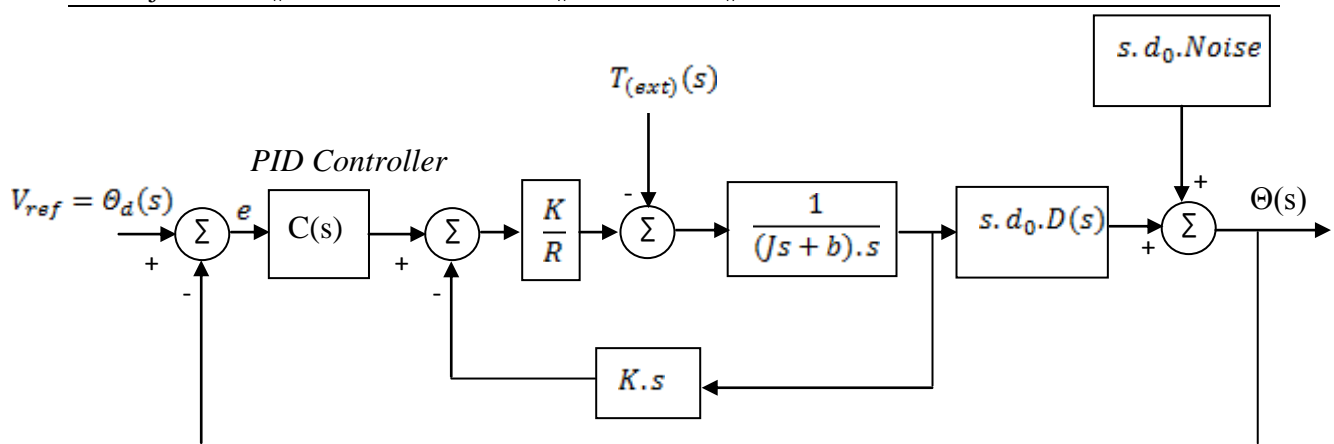


Figure 15: Control structure of the system

The controller of choice in this research work is Proportional Integral plus Derivative (PID) controller.

### 3.7 The PID Controller

PID controllers are commonly used in a broad range of controller applications and thus the most widely used controller in industry. The PID controller structure is shown in figure 16. The parameters ( $K_p$ ,  $K_i$ ,  $K_d$ ) will be tuned using SIMULINK PID tune tool.

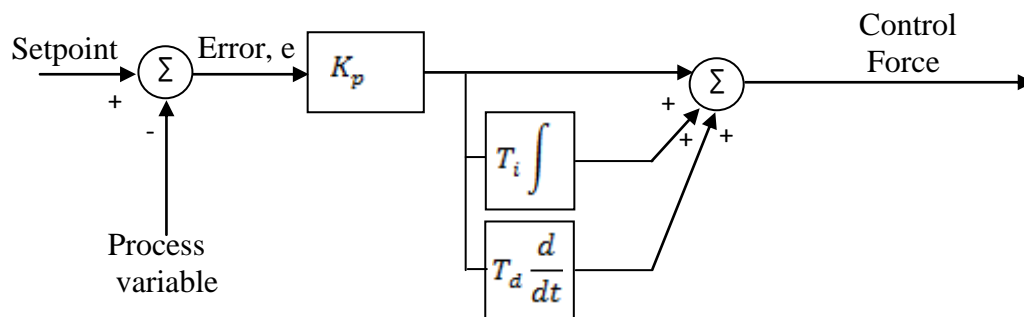


Figure 16: PID control structure

$$\text{In time domain, the PID control force } u(t) = K_p \cdot e + K_i \int e dt + K_d \frac{de}{dt} \quad (19)$$

Where  $e$  is the error in measurement,  $K_p$  is the proportional constant,  $K_i$  is the integral constant,  $K_d$  is the derivative constant

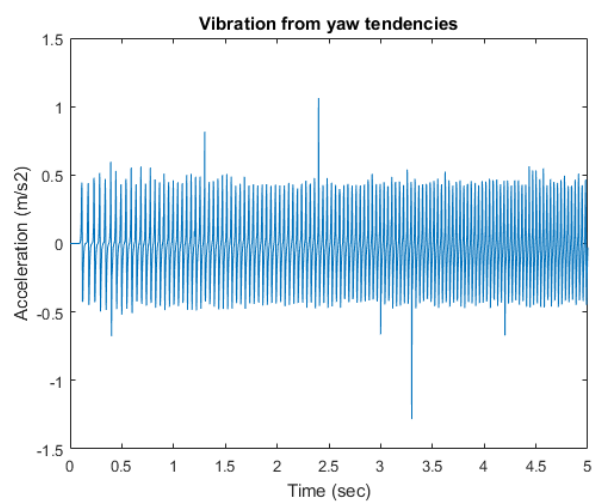
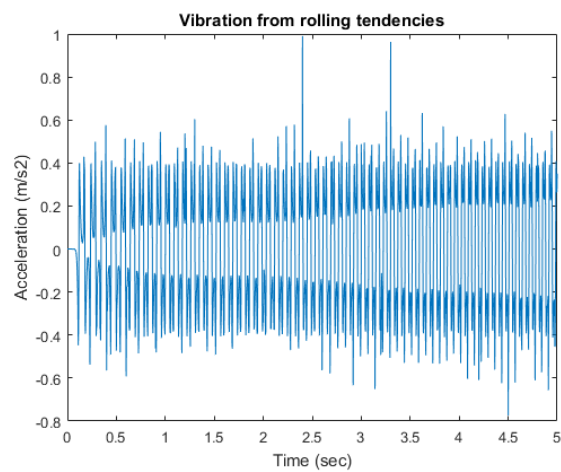
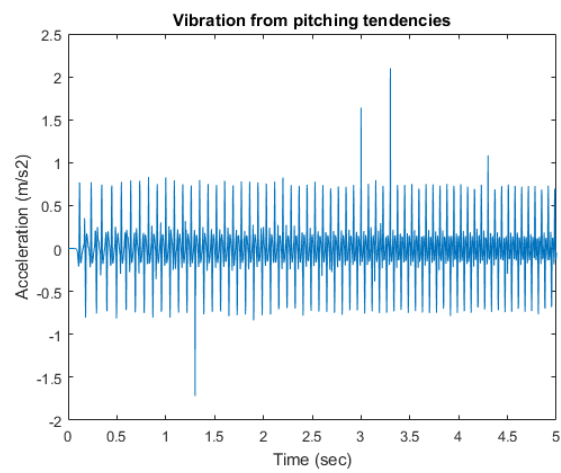
In frequency domain, by Laplace transform, the transfer function for the controller will be

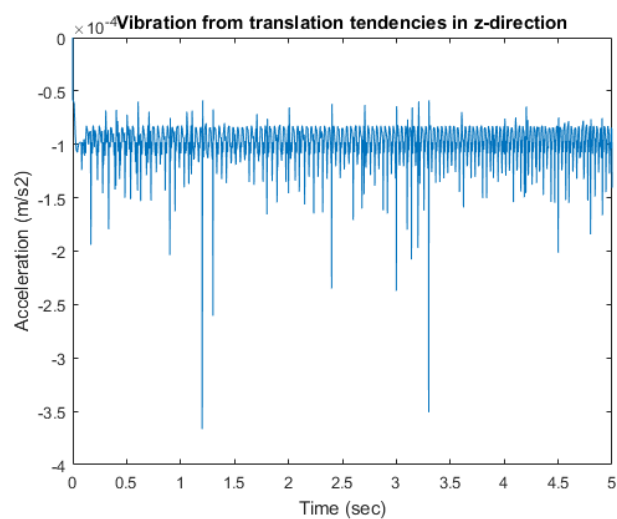
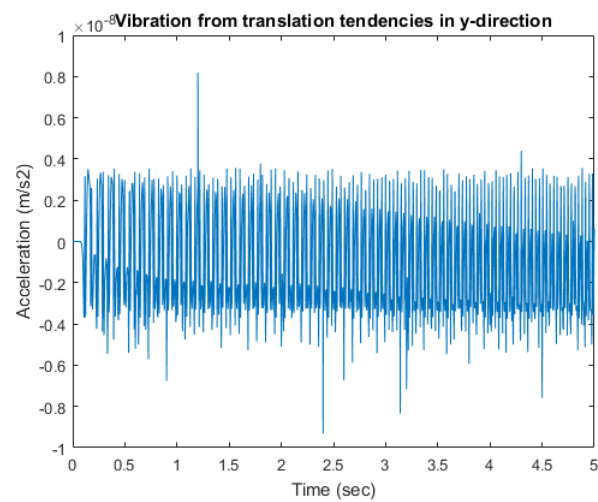
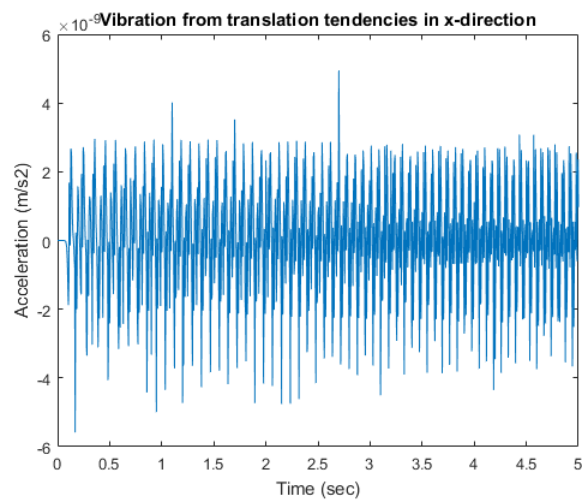
$$U(s) = \left( K_p + \frac{K_i}{s} + sK_d \right) E(s)$$

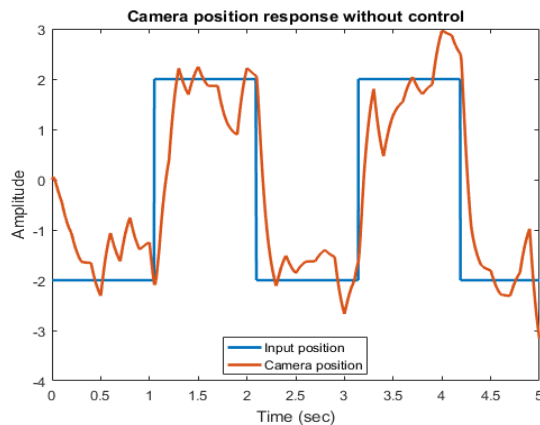
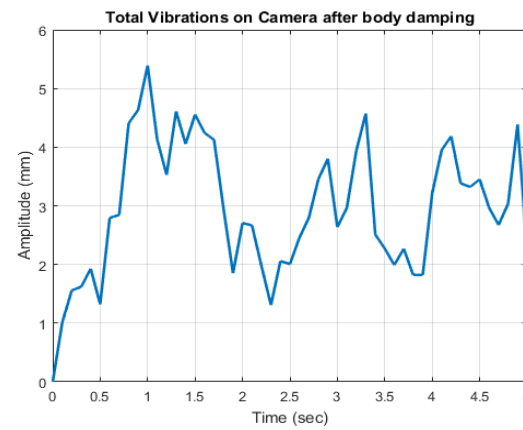
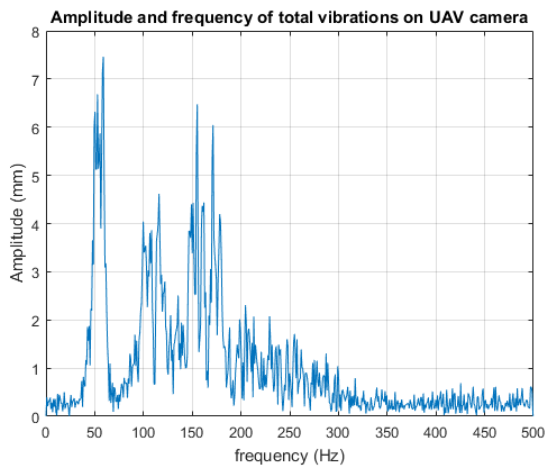
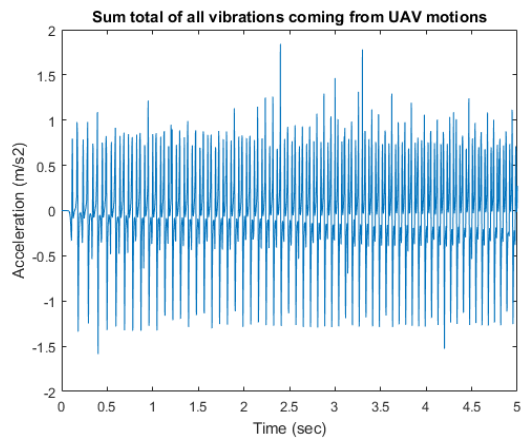
$$C(s) = \frac{U(s)}{E(s)} = K_p \left( 1 + \frac{1}{T_i s} + sT_d \right) \quad (20)$$

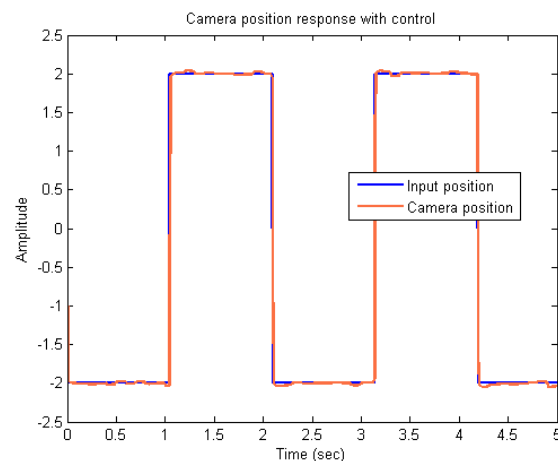
$T_i$  is the integral time constant,  $T_d$  is the derivative time constant

### 3.8 Results









### References

- [1]. Control Tutorials for MATLAB and Simulink - Motor Position System.mht
- [2]. Henri Eisenbeiss (2004). Institute for Geodesy and Photogrammetry, ETH-Hoenggerberg, CH- 8093, Zurich, Switzerland, International Workshop on Processing and visualization using high-resolution imagery, Pitsanulok, Thailand.
- [3]. G. Nicolás Marichal Plasencia, María Tomás Rodríguez, Salvador Castillo Rivera and Ángela Hernández López(2012), Modeling and Analysis of Vibrations in a UAV Helicopter with a Vision System, International Journal of Advanced Robotic Systems.
- [4]. Hu R., Shi R., Shen I., and Chen W. (2007) Video Stabilization Using Scale-Invariant Features. The 11th International Conference Information Visualization, pp. 871-877.
- [5]. [https://en.m.wikipedia.org/wiki/unmanned\\_aerial\\_vehicle](https://en.m.wikipedia.org/wiki/unmanned_aerial_vehicle)
- [6]. Jens Windau and Laurent Itti (2011). Multilayer real time video image stabilization. IEEE/RSJ International Conference on Intelligent Robots and system, pp. 2397-2402
- [7]. Marynel Vazquez and Carolina Chang, *IEEE International Conference on Systems, Man, and Cybernetics*, pp. 4019-4024, 2009.
- [8]. Pipatpaibul, Pong-In, "Quadrotor UAV control : online learning approach" (2011). *Theses and dissertations*. Paper 769.
- [9]. [www.lumenera.com](http://www.lumenera.com)
- [10]. Yue Wang, ZuJun Hou, Kariato Leman and Richard Chang (2011). Real-Time Video Stabilization for Unmanned Aerial Vehicles Institute for Info comm Research, A\*Star (Agency for Science, Technology and Research), Singapore.